Kinesin Illuminated

Prevo, B.

2015

Chapter 2.3

FÖRSTER RESONANCE ENERGY TRANSFER AND KINESIN MOTOR PROTEINS

2.3.1 Abstract

Förster Resonance Energy Transfer (FRET) is the phenomenon of non-radiative transfer of electronic excitations from a donor fluorophore to an acceptor, mediated by electronic dipole-dipole coupling. The transfer rate and, as a consequence, efficiency depend non-linearly on the distance between donor and acceptor. FRET efficiency can thus be used as an effective and accurate reporter of distance between two fluorophores and changes thereof. Over the last 50 years or so, FRET has been used as a spectroscopic ruler to measure conformations and conformational changes of biomolecules. More recently, FRET has been combined with microscopy, ultimately allowing measurement of FRET between a single donor-acceptor pair. In this review, I will explain the physical foundations of FRET and how FRET can be applied to biomolecules. The power of the different FRET approaches will be highlighted by focusing on applications to the motor protein kinesin, which undergoes several conformational changes driven by enzymatic action, that ultimately result in unidirectional motion along microtubule filaments, driving active transport in the cell. Single-molecule and ensemble FRET studies of different aspects of kinesin have provided numerous insights in the complex chemomechanical mechanism of this fascinating protein.

INTRODUCTION

Many proteins function by undergoing specific, structural transitions, controlled by their own enzymatic activity (1). To fully appreciate the behavior of such proteins one has to understand in molecular detail how different conformational states contribute to overall protein activity. Kinesins are examples of proteins that go through several distinct transformations repetitively, coupled, on the one hand, to ATP hydrolysis and, on the other hand, to well-controlled mechanical action (2, 3). Different classes of kinesin motor proteins have been discerned, with crucial functions in intracellular transport along the microtubule network of the cytoskeleton, cell division, and microtubule maintenance. In this chapter I will mainly focus on Kinesin-1, the first member of the kinesin superfamily to be discovered and one of the most studied motor proteins. Kinesin-1 (in the following also called kinesin), is involved in active cargo transport in axons. It is a tetrameric protein consisting of two heavy and two light chains (4). The two identical heavy chains form a coiled-coil stalk, with, on the one end, the tail domains responsible for cargo binding and autoinhibition, and, on the other, two motor domains coupled to the stalk via the neck linkers. The motor domains are responsible for microtubule binding, ATP hydrolysis and the conformational changes driving motility (3). After encountering a microtubule, the motor domains alternatingly take 16-nm steps in a hand-over-hand manner, tightly coupled to the hydrolysis of one ATP molecule, while docking on and undocking from well-defined binding sites on the microtubule, resulting in 8 nm steps of the motor's center of mass (Fig. 1) (5). Precise coordination between the binding/unbinding and ATP hydrolysis of the two motor domains allows kinesin to take more than a hundred steps before detaching from the microtubule, a property called processivity (2, 5). At cellular ATP concentrations, kinesin runs with a velocity of about 800 nm s^{-1}. Consequently, a motor domain has on average ~10 ms to go through the successive structural and enzymatic transitions underlying a single step.

Many aspects of our knowledge about kinesin structure and enzymology have been obtained with ensemble biochemistry techniques, electron microscopy and X-ray structural analysis. These studies have revealed crucial insights in kinesin's ATPase kinetics, microtubule-binding properties and conformations. Crucial for unraveling kinesin-driven motility has been the development of *in vitro* motility assays (3), which allow direct observation and quantification of kinesin's

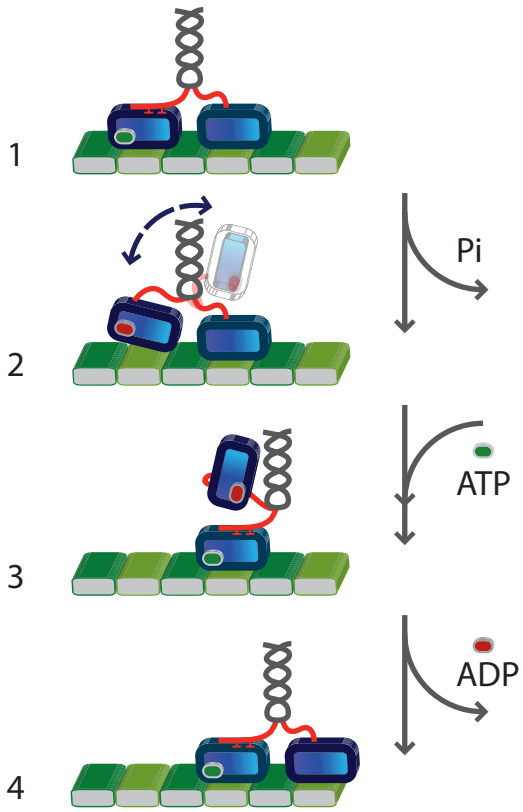

Figure 1: Minimal model of the kinesin mechanochemical cycle (30). Kinesin is represented by the two motor domains (blue), neck linkers (red) and connecting coiled coil; ATP is depicted by the green oval, ADP by the red oval; the green and grey structure on the bottom is a microtubule protofilament. In state 1 both motor domains are microtubule bound, the leading motor domain is nucleotide free, while the trailing one has ATP bound. The neck linker of the trailing head is docked and pointing forward, while that of the leading head is undocked. After ATP hydrolysis and release of inorganic phosphate, the trailing motor domain detaches from the microtubule track and its neck linker undocks (state 2). The subsequent binding of ATP to the leading head results in forward docking of its neck linker, resulting in a relatively compact configuration of the two motor domains (state 3). The trailing, ADP-bound motor domain moves forward, binds to the next available binding site on the microtubule, releasing ADP (state 4). The motor domains have now swapped leading and trailing roles and the system is in the initial configuration.

motility parameters under well-controlled conditions. Early motility assays probed the concerted action of multiple kinesin motors acting on a single microtubule. Later assays allowed study of motion and force development of individual kinesins. Single-molecule techniques provide crucial advantages for the study of dynamics of biomolecules: they allow resolution of population heterogeneity, do not require synchronization of enzymatic action (like ensemble chemical kinetics measurements) and allow correlation of different properties of the biomolecule of interest (6). More importantly, they allow for the direct observation of the behavior of single motor proteins, such as kinesin, proteins that *in vivo* also can act on their own or in small numbers. Two single-molecule techniques have been instrumental in unraveling the mechanism of kinesin (7). First, optical tweezers experiments allow measurement and application of forces exerted by the motor (in the picoNewton range), while at the same time recording its displacement with nanometer resolution. Using this technique, the maximum force a single kinesin can exert has been determined (~6 pN), as well as its step size (8 nm) and velocity and other motility parameters under mechanical load (8, 9). The second single-molecule technique that has changed our understanding of kinesin motility is single-molecule fluorescence microscopy. This technique allows direct visualization of kinesin processivity (10) and has been instrumental in demonstrating that kinesin's two motor domains step in a hand-over-hand fashion, making 16 nm steps one after the other (11).

Crucial conformational changes driving kinesin motility, however, take place on the (sub)millisecond time scale and nanometer length scale, which are difficult to access with optical tweezers (which typically only provides insight in the overall behavior of the dimeric motor) and standard single-molecule fluorescence microscopy techniques (which lack both time and spatial resolution) (7). There is, however, a fluorescence-based technique that is particularly well suited to fulfill the requirements necessary to gain access to these fast and minute structural transitions: Förster Resonance Energy Transfer (FRET) (12, 13). In FRET, the transfer of electronic excitations from a donor fluorescent probe to an acceptor is measured, allowing quantitative distance measurements in the 1-10 nm length range, with a sub-millisecond time resolution. FRET, which can be used in ensemble and single-molecule measurements, is thus ideally suited to shed light on protein conformational changes and has been applied extensively to dissect the mechanism of kinesin stepping.

In this chapter I will review how FRET studies on the ensemble and single-molecule level have contributed to our understanding of kinesin function. First, the physical foundations of FRET will be introduced and its capabilities and limitations described. Next, it is discussed how FRET can be used to study biomolecule conformational changes in ensemble experiments, in cuvette and under the microscope, and in single-molecule experiments. Finally, I will review how FRET has been applied to unravel kinesin's mechanism and function by highlighting distinct aspects of the kinesin mechanism: ATP hydrolysis, neck-linker conformational changes, stepping and conformational changes regulating motor activity. FRET studies have been successfully applied to shed light on these diverse aspects of kinesin function. By highlighting the insights FRET studies have provided in kinesin motility, I hope to convince the reader that FRET is a powerful tool to quantitatively dissect structural and conformational changes of biomolecules in general, which are crucial aspects for understanding their function, activity and mechanism.

FÖRSTER RESONANCE ENERGY TRANSFER

FRET is a physical phenomenon that has been successfully used as a molecular ruler to study changes in distance (on the several nanometers length scale) and relative orientation (14). FRET can occur when two fluorophores are close enough to transfer excitations via electronic coupling of the transition dipole moment of the donor fluorophore to the absorption transition dipole moment of the acceptor. FRET can be readily measured in standard bulk fluorescence experiments, but is also accessible using fluorescence microscopy, including single-molecule fluorescence spectroscopy. In the following I will describe the physical mechanism of FRET and how it can be used to obtain insight into biomolecule conformational changes, using bulk experiments, fluorescence microscopy and single-molecule approaches.

PHYSICAL BACKGROUND

2.3.2 Strong coupling: excitons

When two fluorophores come close, they can alter each other's electronic properties (12). At short distances (for organic fluorophores in a watery environment, less than a few nanometers), the electronic coupling between the transition dipole

moments of the optical transitions of the molecules can be strong, resulting in so called exciton splitting of the excited states: the energy of the original excited states is shifted, while the oscillator strength of the individual transition is redistributed. This leads to altered spectra with shifted peaks with altered intensity. When such a strongly coupled system of fluorophores is excited with light, the excitations are delocalized over the coupled molecules and called excitons: the excitation energy is almost instantaneously distributed over the molecules. Exciton coupling can occur between identical as well as different molecules. It can result in increased or decreased absorption at a given wavelength, depending on the orientation of the transition dipole moments with respect to each other and the axis connecting the molecules (12). It also has an effect on the fluorescence emitted after excitation. The fluorescence quantum yield can increase (superradiance) or decrease (quenching). This effect can be used to measure conformational changes altering the distance between two fluorophores attached to a biomolecule in the sub- to a few nanometers range. It should be noted that very short distances between the fluorophores are required and that it is difficult obtain quantitative information on the actual distances.

2.3.3 Weak coupling: Förster Resonance Energy Transfer

In the weak coupling limit (which occurs when the coupling energy is much less than the spectral band width) no changes in the absorption spectrum of the pair of fluorophores can be discerned (13). When one of the molecules is excited, however, non-radiative transfer of the excitation from this molecule to the other can take place in case the energy differences match and the coupling energy is large enough (Fig. 2A, B). Because of the non-radiative nature of the excitation transfer we encourage the explanation of the 'F' in FRET to be an abbreviation of 'Förster' instead of 'Fluorescence' as frequently used, since the latter might be confusing in this respect. For the case of dipole-dipole coupling (for strongly absorbing and emitting fluorophores, as discussed here, the most relevant case) Theodor Förster derived the following formula for the transfer rate (k_T) between an excited donor (D) and an acceptor fluorophore (A) (13, 15):

$$k_T = \frac{1}{\tau_D^0}\left(\frac{R_0}{r}\right)^6 \tag{1}$$

where τ_D^0 is the fluorescence lifetime of the donor in the absence of the acceptor,

r the distance between the fluorophores and R_0 the so-called Förster distance (the donor-acceptor distance at which the transfer rate is equal to $1/\tau_D^0$). Note that the rate of transfer is inversely proportional with the inter-fluorophore distance to the power six, a signature of dipole-dipole coupling (Fig. 2C). The transfer efficiency (Φ_T) can be expressed as (13):

$$\Phi_T = \frac{k_T}{1/\tau_D^0 + k_T} = \frac{1}{1 + (r/R_0)^6} = 1 - \frac{\tau_D}{\tau_D^0} \tag{2}$$

where τ_D is the fluorescence lifetime of the donor in the presence of the acceptor. Equation 2 provides another definition of the Förster distance: the donor-acceptor distance at which the transfer efficiency is 50%. The Förster radius (in Ångstrom) can be found using (13):

$$R_0^6 = \frac{9000\,(\ln 10)\,\kappa^2 \Phi_D^0}{128\pi^5 N_{Avo} n^4} J\,(\lambda) = 8.79 \times 10^{-5} \kappa^2 \Phi_D^0 n^{-4} J\,(\lambda) \tag{3}$$

where Φ_D^0 is the fluorescence quantum yield of the donor in the absence of the acceptor, N_{Avo} Avogadro's number, n the refractive index of the medium, $J\,(\lambda)$ the overlap integral describing the degree of overlap between donor fluorescence emission spectrum and acceptor absorption spectrum (Fig. 2B), and κ^2 the orientation factor, a measure for the relative orientation of the transition dipole moments of donor (emission) and acceptor (absorption) and the vector connecting the molecules (Fig. 2D). The overlap integral is given by (13):

$$J\,(\lambda) = \int_0^\infty I_D\,(\lambda)\,\varepsilon_A\,(\lambda)\,\lambda^4 d\lambda \tag{4}$$

where λ is the wavelength, $I_D\,(\lambda)$ the donor fluorescence emission spectrum, $\varepsilon_A\,(\lambda)$ the acceptor absorption spectrum (both with area under the spectrum normalized to unity). The better the overlap between acceptor absorption and donor emission spectra, the larger the overlap integral is and the larger the Förster distance (see Fig. 2B).

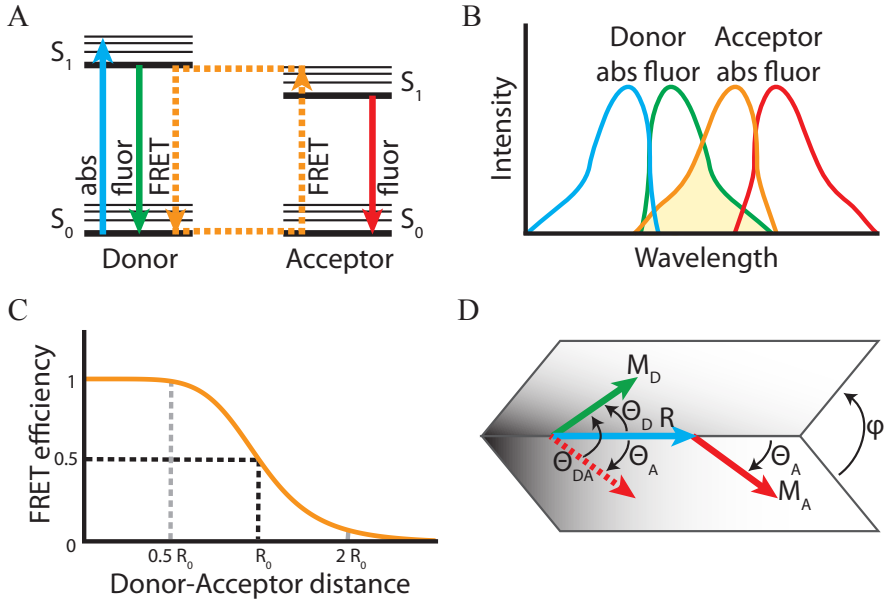

Figure 2: Förster Resonance Energy Transfer (FRET). (A) Minimal energy diagram representing the first two singlet electronic levels of a donor and acceptor fluorophore. Absorption of a photon (abs; cyan arrow) results in excitation of the molecule from the lowest vibrational level (thin black horizontal lines represent the vibrational levels) ground state (S_0) to higher vibrational levels of the first excited state (S_1). This donor excited state can decay to the ground state via fluorescence (fluor; green arrow). As an alternative, the donor excited state can be transferred nonradiatively to the acceptor via FRET (dashed orange arrows). The acceptor excited state can decay to the ground state via emission of fluorescence (fluor; red arrow). **(B)** Absorption (abs) and fluorescence emission (fluor) spectra of donor and acceptor. FRET requires overlap between donor emission and acceptor absorption spectra (yellow area). **(C)** Graph of FRET efficiency as a function of donor-acceptor distance. At R_0, the Förster distance, energy transfer efficiency is 50%, at ½R_0 98.5% and at 2R_0 1.5%. **(D)** Schematic depiction of the vectors and angles involved in determination of the FRET orientation factor κ^2: the transition dipole moments of donor emission (M_D, green) and acceptor (M_A; green), the connecting vector (R; cyan), Θ_{DA} the angle between M_D and M_A, donor emission and acceptor absorption dipole moments, Θ_D and Θ_A the angles between the respective dipole moments and R, and φ the angle between the planes formed by R and each of the two dipole moments.

In addition the Förster distance depends strongly on κ^2 (the orientation factor) (13):

$$\begin{aligned}\kappa^2 &= (\cos\Theta_{DA} - 3\cos\Theta_D\cos\Theta_A)^2 \\ &= (\sin\Theta_D\sin\Theta_A\cos\varphi - 2\cos\Theta_D\cos\Theta_A)^2\end{aligned} \quad (5)$$

where Θ_{DA} is the angle between donor emission and acceptor absorption dipole moments, Θ_D and Θ_A the angles between the respective dipole moments and the vector (R) connecting the fluorophores, and φ the angle between the planes formed by vector R and each of the two dipole moments (Fig. 2D). The orientation factor is 0 when the two dipoles are oriented perpendicular, 1 when they are parallel, but both perpendicular to the connecting vector, and 4 when they are parallel with each other and the connecting vector. The orientations of the dipoles are often not known. In case they are random, but fixed in time the ensemble average of κ^2 can be assumed to be 0.476; in another case when they are rotating fast on the timescale of fluorescence (nanoseconds) the time average of κ^2 can be assumed to be ⅔. For calculating the Förster distance, often ⅔ is used. Depending on the combination of fluorophores, Förster distances typically range from 20 to 90 Å (16), making FRET an excellent method to obtain distances and changes in distance in the range of several nanometers. The FRET efficiency scales highly non-linear with r (Fig. 2C): when the fluorophores are $½R_0$ apart the efficiency is 0.985 and when they are $2R_0$ apart 0.0154. In order to make use of FRET to obtain insight into biomolecule conformational changes, care has to be taken to carefully select donor and acceptor pair (i.e. Förster distance) and labeling positions on the biomolecule of interest in order to be in this sensitive (= steep) part of the FRET efficiency curve (Fig. 2C) (13). In most cases this requires that a sufficient amount of information is available on the structure of the biomolecule and the conformational changes of interest. To improve the chance of success, it is wise to select several different labeling locations, since fluorescent labeling can result in altered properties of the biomolecule (this has to be checked always) and conformational changes can in reality be different than what is inferred from crystal structures or other approaches. Accurate placement of labels requires specific attachment to the biomolecule of choice. In most *in vitro* cases synthetic organic dyes are used such as the Alexa Fluor (Invitrogen) or Cy dyes (GE Healthcare) because of their superior fluorescence properties and relatively small size. For nucleic acid labeling, diverse types of fluorescent nucleotides can be readily incorporated using automated solid-state synthesis (17). In the case of protein labeling, in many cases cysteine-reactive labels are used (17). Note that

attaching a donor and an acceptor is difficult to achieve in a specific way (i.e. donor in one location, acceptor in another). This can in some cases be tolerated. If a higher degree of control is necessary more advanced labeling strategies involving inteins or non-natural amino acids in combination with *in vitro* translation are required (17). For *in vivo* measurements other strategies have been employed, including fusions of the protein of interest and a fluorescent protein (18). It should be noted that fluorescent proteins are not well suited for single-molecule FRET because of their size and limited photostability (19). Novel technologies make use of fusion proteins that specifically and covalently bind membrane permeable synthetic, fluorescently labeled substrates, such as the SNAP- and CLIP-tags from New England BioLabs Inc.

HOW TO MEASURE FRET

Once the biomolecule of interest is specifically and correctly labeled, its conformational changes can be monitored by measuring the FRET efficiency, for example as a function of time (20). Changes in FRET efficiency can then be converted to changes in donor-acceptor distance and/or orientation. Many conformational changes in proteins or DNA take place on the microsecond to second timescale, much slower than the nanosecond time scale of the FRET process itself. FRET can and has been used as an effective molecular ruler, but this is by far not trivial since for accurate and absolute distance measurements detailed information on orientations is required (21, 22, 23). Such signals can be obtained both in bulk, for many FRET pairs simultaneous, but also for single pairs. Below further technical implementations are discussed. FRET can be measured in bulk solution, spatially resolved in a fluorescence microscope and on single molecules. These three modalities will be discussed in more detail below.

2.3.4 Ensemble experiments

A straightforward way to measure FRET is to measure it on a solution of the biomolecule of interest using a fluorimeter (16, 20). The FRET efficiency can then be determined from the emission spectrum obtained upon donor excitation (i) by taking the ratio between acceptor fluorescence intensity and the sum of donor and acceptor fluorescence intensities or (ii) by determining the relative changes of donor emission intensity in the presence and absence of acceptor. The first approach requires careful correction of the signals for (relative) detection

efficiencies, fluorescence quantum yields and spectral overlap of excitation and emission spectra (24). The latter approach does not depend on these corrections, but requires accurate knowledge of the intensity in the absence of the acceptor, which can be non-trivial.

Such experiments are in principle steady-state experiments. Even when a biochemical reaction takes place in the sample involving conformational dynamics that in principle could result in temporal changes in FRET, ensemble averaging over non-synchronized transients will result in a static, population-averaged FRET value. Population-averaged transients can be measured though, when a non-equilibrium situation is created for example by mixing solutions to start the biochemical reaction in a synchronized way over the whole ensemble of biomolecules (16). Such mixing can be done very fast (mixing times down to about a millisecond), using dedicated stopped-flow equipment. In a stopped-flow experiment, one typically refrains from measuring the full spectrum, but instead measures the total fluorescence intensity in two (donor and acceptor) or one (donor) spectral channels. An important disadvantage of this approach is that usually substantial quantities of proteins are used for only a single reaction cycle.

2.3.5 FRET microscopy

FRET measurements can be performed using a microscope in order to obtain spatially resolved signals, for example in a living cell. This can be a very powerful approach for example to determine local Ca^{2+} concentrations using FRET-based sensors (16). Crucial in such studies is to correct the fluorescence signals well for spectral overlap and detection efficiencies. Two potential, additional sources of artifacts are photobleaching (due to the much higher excitation intensities used) and unknown concentrations of biomolecules containing donor and acceptor. The most successful methods to measure FRET in bulk using microscopes are based on determining the fluorescence lifetime of the donor molecules and comparing those to the fluorescence lifetime of the donor in absence of the acceptor. In contrast to fluorescence intensity, fluorescence lifetime is a quantity hardly affected by protein concentration and factors such as spectral overlap and detection efficiency. More details of fluorescence lifetime imaging (FLIM) and its use for FRET measurements can be found elsewhere (25).

2.3.6 Single-molecule FRET

Ensemble FRET experiments are obtained by averaging the properties of all molecules in the sample and thus cannot provide direct insight in potential conformational heterogeneity of the biomolecules under study (6, 26). Furthermore, to obtain temporal information on changes in FRET, all molecules in the sample need to be synchronized, which is not always possible and often requires large quantities of biomolecules. These limitations can be overcome by measuring FRET on single donor-acceptor pairs (smFRET) (27). Crucial in smFRET is that the fluorescence is detected with high efficiency and that background signals are well suppressed. smFRET does not work with all fluorophores: the amino acid tryptophan, commonly used as donor in stopped-flow FRET experiments is not bright enough and fluorescent proteins, commonly used with FRET-FLIM, are not photostable enough and their fluorescence intensities fluctuate too much (19). In practice, only synthetic dyes such as Alexa Fluor (Invitrogen), Cy (GE Healthcare) and Atto (Attotec) are used for smFRET. Different experimental approaches, with different areas of application are widely used to measure FRET on single donor-acceptor pairs.

In one implementation, a confocal microscope is used, with a static laser focus in a solution with freely diffusing fluorescently labeled molecules of interest (28). Only when biomolecules are present in the confocal volume, fluorescence will be emitted. When the biomolecule is labeled with a donor and acceptor and the donor is excited, donor and acceptor fluorescence can be detected, depending on FRET. Using this method, in a short time, the FRET signal of many molecules can be measured allowing accurate measurement of histograms of the FRET efficiency, directly probing heterogeneous conformation distributions. A drawback of many FRET experiments is that it is very difficult to obtain samples with a donor and acceptor labeling efficiency of 100%, resulting in multiple, overlapping FRET populations, which makes interpretation of the data difficult. To overcome this problem, the ALEX (Alternating Laser Excitation) method has been devised, which involves fast switching between donor and acceptor excitation (29). Using ALEX, for each freely diffusing molecule not only the FRET efficiency can be determined, but also the donor-acceptor stoichiometry, which allows filtering out molecules that lack either donor or acceptor. The disadvantage of burst approaches (including ALEX) is that they do not provide insight in temporal changes of the fluorescence signals, since each molecule is probed only for the brief residence

time in the confocal volume. A modification of this approach has been applied to measure FRET on moving kinesin motors (30). Here, the laser exciting the donor fluorophore was focused on a microtubule fixed to a cover glass. Fluorescence signals from individual kinesins walking over the microtubule and through the confocal spot can be measured in time for the duration of the transit (about a second), with an effective time resolution of 100 microseconds (31). Fluorescence time traces obtained in this way can be analyzed using auto- and cross-correlation analysis. ALEX was not necessary to discriminate donor and acceptor labeled motors from partly labeled ones, since the fluorescence intensity time traces provide enough insight to allow accurate filtering on the basis of donor and acceptor intensities.

Another approach to measure smFRET is based on wide-field fluorescence microscopy. In this approach, a region (with a typical size of several to several tens of micrometers) of the sample is illuminated using epi-illumination or total-internal-reflection illumination (TIRF) (32). In epi-fluorescence microscopy a large part of the sample volume is illuminated, which can result in unwanted background signals originating from above or below the image plane. In TIRF, this problem is solved by illuminating only a thin region of the sample (approximately one hundred nanometers), close to the cover-slip/sample interface, with the evanescent wave of a totally internally reflected laser beam. Irrespective of the illumination method, the fluorescence emitted by the sample is detected with a camera, allowing inspection of a whole region of the sample (and many individual molecules) in a single shot, lasting typically in the range of 10 ms to 1 s. Care needs to be taken to choose the frame integration time such that movement of the fluorophores of interest does not result in motion blurring. In a typical application to kinesin, microtubules are attached to the cover glass and fluorescent motor proteins are added to the solutions. When freely diffusing, the motors will move fast and randomly, resulting in a diffuse background fluorescence signal. Only when they bind to a microtubule and move along it, clear and localizable spots can be observed in the images. In order to measure FRET signals, donor and acceptor fluorescence intensity is measured by spectrally splitting the emission signal and imaging it on two cameras or side-by-side on a single one. The advantage of this approach is that multiple biomolecules can be followed in time at the same time. The total duration the motors can be observed is limited by photobleaching of the fluorescent probes or the time they remain attached to the microtubules (run length). The time resolution of this approach is limited

by the frame acquisition time of the camera, which is at most about 100 Hz (depending on fluorescence intensity).

USING FRET TO DISSECT THE MOTILITY MECHANISM OF KINESIN

As discussed above, FRET is ideally suited to obtain detailed insight in the conformations of biomolecules. In addition, smFRET allows resolution of conformational heterogeneity and of the time scales of interconversion between different conformations, without the need to synchronize the ensemble of biomolecules under study. As a consequence smFRET has been applied to many different biological problems, ranging from the conformation of DNA (23), the folding of RNA (24) and proteins (33), to the different conformations of RNA polymerase during different stages of its catalytic activity (34). In this chapter I will provide an overview of the use of FRET, in particular in its single-molecule form, to motor proteins of the kinesin superfamily. Kinesin is a particularly interesting subject for FRET measurements since it undergoes changes in conformation in a repetitive, cyclic way, resulting in forward motion. Kinesin's mode of action involves the hydrolysis of ATP, tightly coupled to conformational changes, binding to and unbinding from the microtubule lattice and stepping. In addition, a large-scale conformational change of the cargo-binding tail of the protein is an important means of regulation of the protein. In the remainder of this contribution I will review FRET studies that have addressed these important features of kinesin's mode of action. The different FRET approaches that have been taken are schematically summarized in Figures 3 and 4. In Figure 3 labeling locations are depicted in the kinesin overall structure, while the different FRET approaches applied are depicted in Figure 4.

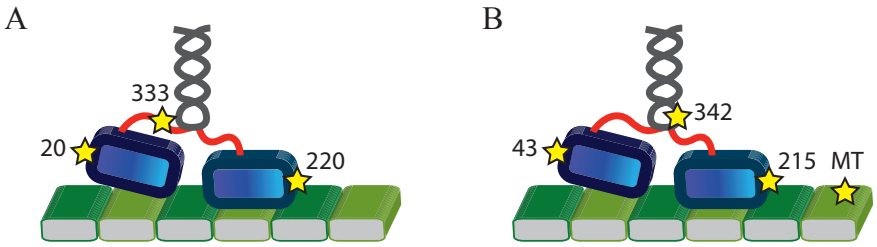

Figure 3: Kinesin structure with labeling locations of FRET studies discussed indicated (30, 41, 44, 45, 46, 47, 51, 54).

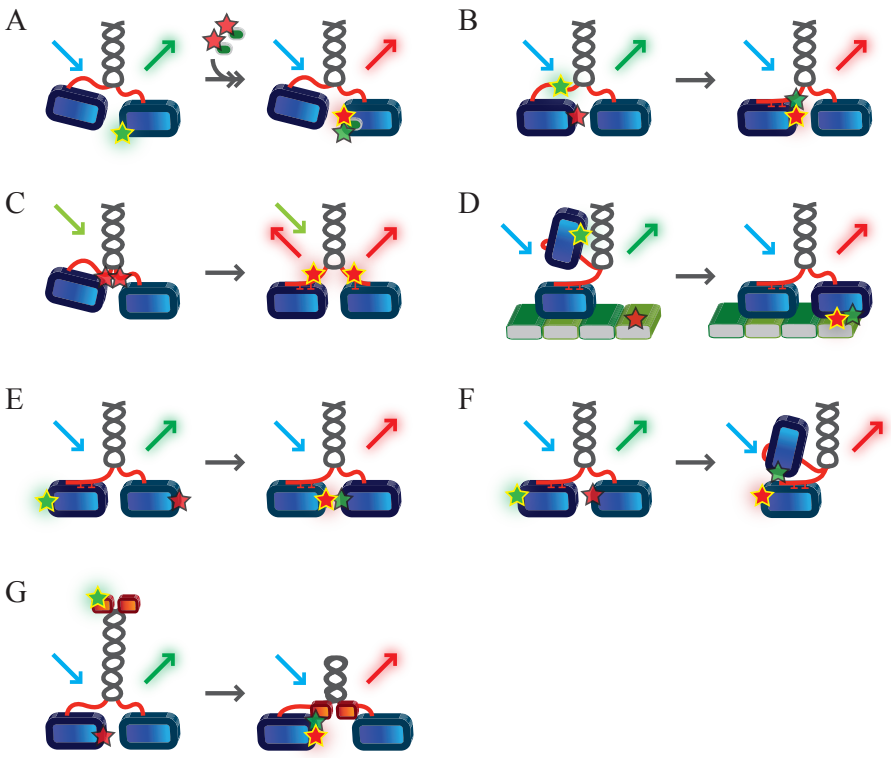

Figure 4: Schematic representations of FRET geometries applied to kinesin. Donor is represented by green asterisk, acceptor by red asterisk, donor excitation by cyan arrow, donor fluorescence by green arrow and acceptor fluorescence due to FRET by red arrow. **(A)** FRET between donor on kinesin motor domain and acceptor on ATP (41, 41). **(B)** FRET between donor on neck linker and acceptor on the same motor domain (44, 47). **(C)** Exciton formation resulting in fluorescence quenching of two fluorophores attached to both neck linkers (46). **(D)** FRET between donor on motor domain and acceptor on microtubule (51, 53). **(E)** FRET between donor on one motor domain and acceptor, in another location, on the other motor domain (54). **(F)** FRET between donor on one motor domain and acceptor, in the same location, on the other motor domain (30). **(G)** FRET between donor on tail domain and acceptor on motor domain (60). See main text for further explanation.

2.3.7 ATP hydrolysis

The hydrolysis of a single ATP molecule into ADP and inorganic phosphate by kinesin results in a single 8-nm step, kinesin's trailing motor domain stepping 16 nm, from its original binding site on the microtubule, passing the leading domain, to the next available binding site (Fig. 1) (11). Traditionally, the rate of ATP hydrolysis by enzymes such as kinesin is determined in bulk by measuring the formation of ADP or phosphate by means of radioactivity (32P), changes in light absorption (e.g. making use of complex formation between molybdate and phosphate, often in the presence of malachite green, or using a coupled assay involving lactate dehydrogenase and NADH) (35). In order to obtain deeper insight into the binding and release of nucleotides, frequent use is made of the fluorescent nucleotide-analogue MANT-ATP (or MANT-ADP) containing the N methylanthraniloyl chromophore. The fluorescence properties of MANT-nucleotides change substantially upon binding to the enzyme's active site. This, combined with the with MANT fluorescence being measurable in real time with high sensitivity makes them suitable probes to study nucleotide binding, release and protein conformational changes using stopped-flow equipment. Care has to be taken, because the fluorescent moiety slightly alters the rates for binding and hydrolysis of MANT-ATP compared to ATP (36). MANT-ATP has been used to study many different ATP-hydrolyzing proteins, such as myosin. In myosin it was found that the sensitivity of MANT-fluorescence detection can be further enhanced by exciting it by FRET from a tryptophan donor, naturally occurring in the nucleotide binding pocket (37). This particular FRET approach cannot be used for Kinesin-1, since it does not contain tryptophans in its nucleotide binding pocket. Although less efficient, FRET between tyrosine residues and MANT has been used successfully to study ADP release of *Drosophila* kinesin (36). Some kinesins of other families (Kinesin-5 and Kinesin-7), do contain tryptophans close to the ATP binding site and tryptophan-FRET approaches have been used to determine ATP-binding kinetics for these proteins (38, 39). In a particularly interesting approach, Xing and coworkers generated five Kinesin-1 mutants with tryptophan residues introduced at different locations close to the ATP-binding site (Fig. 4A) (40). Using a combination of ensemble steady-state and stopped-flow FRET measurements between tryptophan and MANT-nucleotides and computer modeling of the nucleotide-binding pocket, they obtained evidence for three different nucleotide-bound conformations of kinesin, that mainly show changes in position of the so-called "switch II" loop and helix, which relay

information from the nucleotide binding pocket to the microtubule-binding domain, thus controlling the microtubule affinity in different nucleotide-bound states of the motor.

For many fluorescence experiments, MANT-nucleotide analogues are ideal: their fluorescence properties are reasonably good and the fluorophore is small compared to the nucleotide, hardly affecting nucleotide binding, hydrolysis and release. Unfortunately, MANT's fluorescence properties (in particular fluorescence quantum yield and the UV excitation wavelength) make it inapt for single-molecule fluorescence experiments. Other nucleotide analogues that do allow single-molecule FRET have been used by Verbrugge and coworkers (41). They studied changes in FRET between an Alexa Fluor 555 attached to a unique cysteine introduced in a cysteine-less mutant of Kinesin-1 at position 43 (Fig. 3) and Alexa Fluor 647 ATP (Alexa Fluor 647 2'-(or-3')-O-(N-2-aminoethyl)urethane), Figure 4A. Because of its relatively large fluorophore, this ATP analogue is hydrolyzed by Kinesin-1 with substantially altered kinetics: the maximum velocity decreased more than two-fold, the Michaelis constant increased more than two-fold. Nevertheless, Alexa Fluor 647 ATP is hydrolyzed by Kinesin-1 resulting in processive motility. Use of FRET served two goals in this experiment: (i) it allowed measurements at rather high fluorescent ATP concentrations (up to 40 micromolar), (ii) it allowed discrimination between fluorescent ATP binding to the one donor-labeled motor domain and the unlabeled one. Using the single-molecule confocal fluorescence motility assay discussed before (31), donor fluorescence intensity time traces were obtained showing continuous switching between low (fluorescent ATP bound to non-labeled motor domain) and high FRET states (fluorescent ATP bound to the labeled motor domain) on the time scale of stepping. Traces were analyzed using autocorrelation methods and compared to kinetic models. The data could only be described using models involving alternating-site hydrolysis, in which the two motor domains hydrolyze ATP and step in a sequential way (41).

ATP-hydrolysis by kinesin results in conformational changes in the motor domains that affect microtubule affinity and relative orientation and distance of the motor domains, resulting in forward stepping. Both motor domains are connected to a single coiled-coil stalk via the so-called "neck linkers", ~14-18 amino acids long, highly conserved among plus-end directed kinesins (42). Early electron-microscopy images of *Drosophila* Kinesin-1 showed that one motor domain was always microtubule-bound in the same orientation, irrespective of nucleotide

state, while location and orientation of the other one depended on the nucleotide bound (43). These results suggested that the structural organization of the neck linkers plays an important role in accomplishing asymmetry between the two motor domains. This feature is thought to be crucial for processivity (5), which requires one motor domain to be tightly microtubule-bound while the other steps. In a landmark paper, Rice and coworkers used FRET and other techniques to measure the distance changes between the neck linker and the catalytic core in different nucleotide- and microtubule-binding states (Fig. 4B) (44). They introduced two cysteines at various locations (residue 20, 188, 220, 328 and 333) in monomeric, cysteine-light mutants of human Kinesin-1, which were subsequently labeled with CPM (7-diethylamino-3-(4'-maleimidylphenyl)-4-methylcoumarin) as donor and TMR (tetramethylrhodamine-6-maleimide) as acceptor.

In solution, kinesin monomers labeled at residues 333 and 220 (Fig. 3) did show FRET, with a transfer efficiency of ~85%. The efficiency decreased (to ~76%) when these motors were bound to microtubules in the absence of nucleotides. The efficiency increased (to ~93%), however, when the non-hydrolyzable ATP analogue AMP-PNP was added to the microtubule-bound kinesins, indicating a donor-acceptor distance of less than ~10 Å. Labeling residue 20 instead of 220 gave opposite results, which indicates that the neck linker is positioned away from the tip of the catalytic core in the nucleotide-free microtubule-bound state, while it is located close to the tip of the catalytic core in the nucleotide-bound microtubule-bound state. This substantial structural reorganization of the neck linker in microtubule-bound kinesin motor domains was explained by the neck linker adopting an immobile, docked conformation with ATP bound and a mobile, undocked conformation after hydrolysis and phosphate release. The intermediate FRET efficiency of motor domains in solution suggests that both immobile and mobile neck-linker states can exist when the motor domain is not microtubule bound. A subtle mutation of a well-conserved glycine (G234A) that forms a hydrogen bond with the γ-phosphate of ATP and thus relays information on the status of the nucleotide bound to the microtubule-binding site, did affect neck-linker docking. To determine the particular residues involved in neck-linker conformational changes, Case and coworkers altered amino acids in the neck linker and mutated specific residues in the catalytic core (G291A/G292A) to prevent hydrogen bond formation with the neck linker, in monomeric and dimeric constructs (45). In all these mutants, microtubule-based motility was severely impaired, while the ATPase rate was affected to a lesser extent. Moreover, FRET

measurements on the monomeric, microtubule bound neck-linker mutants with GFP (at the C-terminus of the kinesin construct) as donor and TMR (at position 220) as acceptor (Fig. 3), showed that the FRET efficiency hardly differed between AMP-PNP or no-nucleotide conditions, in contrast to wild-type kinesin. These results indicate that the neck linker hardly affects the motor domain's ATPase rate but is crucial for kinesin motility, conceivably by amplifying minute conformational changes in the nucleotide-binding pocket to large changes in the connecting elements of the motor domains.

Rosenfeld and coworkers used ensemble fluorescence quenching experiments to determine how conformational changes of the neck linkers are connected to stepping (46). They used a dimeric human Kinesin-1 construct, labeled with TMR (tetramethyl rhodamine 5-maleimide) at a cysteine introduced at position 333 (in the neck linker, Fig. 3). The two TMR labels on both kinesin-polypeptide chains are, depending on exact conditions, close enough to form an exciton, resulting in distance-dependent fluorescence quenching (Fig. 4C). They observed that TMR fluorescence intensity was a direct measure of the conformations of the neck linkers: fluorescence intensity was maximal when both neck linkers were docked on their respective motor domains (in the presence of AMP-PNP and microtubules) and substantially quenched when they were both mobile and undocked (in solution without microtubules). These differences in fluorescence intensity were used, in stopped-flow measurements, to determine the rates of the transients between the different states of the kinesin chemomechanical cycle. During processive motion, the fluorescence intensity was intermediate, an observation consistent with the neck linkers switching between docked and mobile configurations, with both motor domains and only one motor domain microtubule-bound respectively.

To gain further insight in the connection between neck-linker conformational changes and processive motility, Tomishige and coworkers performed smFRET measurements on human Kinesin-1 dimers labeled with Cy3 as a donor and Cy5 as an acceptor using TIRF-microscopy (47). A cysteine-light (cysteines other than at the labeling location(s) are replaced) heterodimeric kinesin was created where only one of the motor domains was labeled at positions 215 and 342 (Fig. 3). smFRET measurements on these constructs thus report on neck-linker conformation in one of the two motor domains (Fig. 4B). Two distinct, almost equal populations of motors were observed, one with high and the

other with low FRET efficiency. The high FRET efficiency population is consistent with dimeric motor proteins in which the neck linker of the trailing motor domain is docked and pointing forward, the other, low FRET, population with motor proteins in which the neck linker of the leading motor domain is undocked and pointing backward. At cellular ATP concentrations kinesin stepping results in alternating low and high FRET states, too fast to be observable with wide-field fluorescence microscopy methods. Slowing down the motors by lowering the ATP concentration to ~1 μM allowed resolution of anti-correlated switches in donor and acceptor fluorescence-intensity time traces, directly demonstrating that the neck linker indeed alternates between two different conformations during processive motion of dimeric kinesins. This general result has later been confirmed using single-molecule fluorescence polarization experiments (48). It has remained unclear, however, whether this conformational change is the actual driver of processive motion: the free energy associated to it is only a fraction of that of the hydrolysis of an ATP and it only results in a fraction of the total displacement of a motor domain (5, 49).

2.3.8 Interactions with the microtubule track

A crucial aspect of kinesin processivity is that the affinities of both motor domains for their microtubule binding sites have to be strictly regulated: at any given moment one of the motor domains has to be strongly bound, requiring that the one motor domain is prohibited from dissociating until its partner is bound. Since microtubule affinity and nucleotide state are tightly connected, a motor domains' catalytic activity has to be regulated by its partner's mechanical state (microtubule bound or not). Based mainly on optical tweezers experiments the current idea in the field is that this knowledge is transferred via mechanical strain between the motor domains (5, 50). This aspect of kinesin motility has also been investigated using bulk FRET (51). A cysteine-light and tryptophan-free kinesin construct was used, which was labeled with AEDANS (5-(((2-iodoacetyl)amino)ethyl)-aminonaphtalene-1 sulfonic acid) to a cysteine introduced in the neck linker at position 333 (Fig. 3). With this construct FRET between AEDANS and tryptophans in the microtubule was measured using stopped-flow fluorescence experiments (Fig. 4D). Dimeric constructs were compared with monomeric ones to test whether forward strain on the trailing head increased its dissociation rate. Surprisingly, ATP-induced dissociation of monomeric kinesin was faster than the dissociation of dimeric kinesin's trailing motor domain, indicating that forward

strain does not increase the dissociation rate of this motor domain. Premature dissociation of the leading motor domain could instead be prevented by prohibiting it binding ATP until the trailing head has dissociated. To test this possibility, ATP-binding kinetics were measured using FRET between MANT-ATP and tyrosine residues of the dimeric construct. In the presence of microtubules two binding rates were observed: a fast one corresponding to MANT-ATP binding to the nucleotide-free motor domain and a slow one corresponding to subsequent MANT-ATP binding of the leading motor domain. These results indicated that rearward strain decreases the ATP-binding rate of the leading motor domain by more than tenfold. Looking with a different perspective one could also argue that it is the microtubule that binds the catalytic cores of kinesin and therefore responsible for generating kinesin's intramolecular strain.

Along similar lines, it was suggested that the microtubule E-hooks, the negatively charged C-termini of α-and β-tubulin, can interact with the positively-charged neck of kinesin to enhance processivity (52). To test these ideas, Martin and coworkers used FRET to determine whether kinesin neck and microtubule are indeed close together (53). They generated three dimeric cysteine-light *Drosophila* Kinesin-1 constructs, labeled with Cy5.5 as acceptor at three different locations in the neck. They measured bulk FRET between donor TAMRA-X-taxol bound to the microtubules and the Cy5.5 acceptors on the kinesin (Fig. 4D) and obtained high FRET efficiencies, irrespective of donor location in the neck, indicating that the kinesin neck is orientated in parallel to the microtubule surface. Proteolytic removal of the microtubule E-hooks decreased both kinesin processivity and velocity. FRET efficiency was, however, not affected, suggesting that the neck orientation was not altered. These results suggest that the orientation of the neck is an inherent structural property of Kinesin-1 and is not caused by electrostatic interactions between the neck and the tubulin E-hooks. The parallel orientation might increase the interaction of kinesin with the microtubule to enhance processivity and velocity, and might aid in achieving asymmetry by preventing neck rotation while kinesin walks along the microtubule.

2.3.9 Kinesin's gait: the mechanism of stepping

After discussing how FRET has been applied to study how kinesin hydrolyses ATP, undergoes conformational changes in the motor domain and binds and releases from microtubules, we will now address the actual stepping mechanism.

In the cell, Kinesin-1 steps along microtubules, with a rate of about 100 steps s^{-1} (corresponding to 800 nm s^{-1}). A single step, involving an ATP hydrolysis cycle, release from the microtubule, conformational changes resulting in a step and binding to a next binding site, lasts only 10 ms on average.

One of the crucial questions in the kinesin-stepping mechanism answered by smFRET is the configuration of the two motor domains in the so-called "ATP-waiting state". In this state (state 2 in Figure 1), one motor domain has no nucleotide bound, is tightly microtubule bound and ready to receive an ATP from solution. The other motor domain has ADP bound and is weakly or not microtubule bound. Mori and coworkers addressed this problem by making heterodimeric human Kinesin-1 constructs with Cy3 as donor and Cy5 as acceptor attached to a cysteine on the plus-end side (215) of one motor domain or the minus-end side (43) of the other one (Fig. 3 and Fig. 4E) (54). In the presence of AMP-PNP the FRET efficiency was bimodal, consistent with both motor domains being microtubule bound and each motor domain having equal probability being in leading position. In the presence of ADP, only a single FRET population was observed, indicating that the motors were attached to the microtubules with only one motor domain. At rate-limiting ATP concentrations (2 μM), switches between high and low FRET efficiency could be observed with long dwell times indicating that kinesin spends most of the time with one motor domain bound under these conditions. FRET measurements on kinesin heterodimers with one mutated motor domain incapable of binding to microtubules confirmed these results and also showed that in the ATP-waiting state the ADP-containing motor domain is located behind the other one (i.e. in the minus-end direction) for most of the time. This was confirmed by single-molecule TMR-quenching experiments using the same kinesin construct discussed above (Fig. 4C) (46) showing that the ADP-containing motor domain is located ~8 nm behind the leading one, switching back and forth between a bound and unbound state, with the neck linkers alternating between a separated and joined state (55). A higher temporal resolution was, however, needed in order to dissect the ATP-waiting state at physiological ATP concentrations, where a single mechanochemical cycle takes on average ~10 ms, close to the maximal obtainable time resolution for single-molecule detection using a (EM)CCD camera (32) as used in these studies (54, 55). Verbrugge and coworkers used a confocal fluorescence microscopy based motility assay with submillisecond temporal resolution to measure the time dependence of FRET between kinesin's two motor domains, during

processive motion (30). They created four different homodimeric kinesin constructs with only one cysteine in different locations on both motor domains. These constructs were labeled with Alexa Fluor 555 as donor and Alexa Fluor 647 as acceptor, with a Förster radius of 5.1 nm, which would not result in FRET when both motor domains are microtubule-bound and 8 nm apart (Fig. 4F). Fluorescence intensity time traces were recorded at different ATP concentrations. FRET was observed for only two of the labeling locations (324 and 43; and not for 215 and 149, Fig. 3). Kinetic information was extracted from donor time traces by analyzing their autocorrelations and comparing them to Monte-Carlo simulations. The data could be well described by a 3-state model, with a no-FRET state with both motor domains microtubule bound lasting ~12 ms, an intermediate FRET state with an ATP-concentration dependent duration, the ATP-waiting state, most likely with one motor domain microtubule bound and the other tethered and relatively mobile, and a third low-FRET state lasting ~3 ms with one motor domain microtubule bound and the other oriented in a specific location and orientation, most likely docked to the microtubule-bound motor domain. These and other FRET experiments show that FRET is a powerful tool to measure small distance chances with high temporal resolution, which allows dissecting kinesin's mechanochemical cycle and stepping mechanism.

2.3.10 Autoregulation of kinesin activity

Motor proteins are involved in a wide variety of intracellular processes, for example, the transport of cargo to different locations in the cell. Intracellular transport requires the occurrence of several events to take place in a particular order. First, motors have to dock specific cargo at a specific location, subsequently they have to become active and move along the proper tracks in the proper direction, and finally, they have to unload their cargo at the right moment at the right location. To make it even more complex, motors with different properties often dock onto the same cargo. Therefore, optimal logistics of cargo transport relies on the precise regulation of the motor proteins. *In vitro*, motor action can be regulated by altering the concentration or nature of nucleotides. In the cell, many other essential processes depend on nucleotides and therefore, kinesins have to be regulated in a different way. Early experiments on Kinesin-1 suggested that its motility increased when the motors were attached to a cover glass or microsphere surface. Later experiments indicated that depending on salt concentration full-length Kinesin-1 could exist in two conformations discernible by analytical ultra-

centrifugation, a folded and more extended one (56). On the basis of such experiments it was suggested that Kinesin 1 is only extended and active when cargo is bound to the tail. If no cargo is bound the tail folds back on the motor domains, deactivating them, preventing futile ATP hydrolysis and microtubule binding (57). These ideas have been confirmed using the FRET-based MANT-ADP assays discussed above on *Drosophila* Kinesin-1 heavy chain mutants of different length in- and excluding the light chain (58). These experiments revealed that there is a particular region in the tail, the IAK-homology region that inhibits ADP release from the motor domains. More detailed insight in the stoichiometry of tail motor-domain interactions required for inhibition was obtained by measuring FRET between MANT-ADP and GFP-labeled tail peptides (59). These experiments showed that one tail domain can inhibit both motor domains at the same time *in vitro*.

To test how the activity of Kinesin-1 is regulated *in vivo*, Cai and coworkers monitored kinesin's conformation and subunit stoichiometry using ensemble FRET in COS cells (60). The cells we transfected to express different forms and combinations of kinesin heavy chains (KHCs) and/or kinesin light chains (KLCs). KHCs and/or KLCs were labeled with enhanced Cyan Fluorescent Proteins (mECFP) as donor and Citrine (mCit) as acceptor, at different locations (Fig. 4G). Full-length kinesins containing both KHCs and KLCs did not bind to microtubules upon addition of AMP-PNP and showed a high FRET efficiency between labels on the motor and tail domains, and moderate FRET efficiency between labels on the motor domain and KLC, indicating that inactive kinesins are in a tightly folded conformation *in vivo*. In addition, these inactive kinesins showed a low FRET-efficiency between labels on both motor domains indicating that these are separated. For active kinesins, a moderate FRET-efficiency was observed between labels on motor and tail domains indicating that, in active kinesins, the tail domains are also positioned close to the motor domains, resulting in a differently folded conformation. In addition, these kinesins showed a moderate FRET-efficiency between labels on the motor domains indicating that the motor domains are more closely together. FRET measurements showed that removal of the IAK-homology region resulted in kinesins (KHCs + KLCs) that were still tightly folded with both motor domains pushed apart but were now able to statically bind to microtubules. These results indicate that the IAK-homology region does not regulate the conformation of kinesin, but controls the microtubule binding capability of the motor domains and therefore plays an important role in kinesin

autoinhibition. The IAK-homology region alone is not sufficient for complete autoinhibition of kinesin, since kinesins that have full-length KHCs but lack the KLCs are active *in vivo*. It is very likely that the KLCs are crucial to keep kinesin in the tightly folded conformation when it is not active. Removing the so-called "TPR" (tetratricopeptide) cargo-binding motifs of the KLC using a truncated version (1-176) resulted in an increase in the inter-motor-domain FRET-efficiency, indicating that these TPR domains are responsible for motor-domain separation in inactive kinesin. The FRET-data described above show that kinesin's activity *in vivo* is regulated by tight folding of the tail domain onto the motor domains, that the interaction between the TPR motifs of the tail and the motor domains pushes the latter apart, and that the IAK-homology region plays an important role in controlling the microtubule-binding activity of kinesin. The authors hypothesized that upon activation by cargo binding and an additional activation step, the tail undocks from the motor domains but stays in close proximity. These studies were the first FRET experiments on kinesin in living cells, providing detailed insight in the conformational changes involved in the regulation of motor activity.

SUMMARY AND OUTLOOK

FRET studies using ensemble and single-molecule approaches, *in vitro* and *in vivo* have provided substantial insight in the complex working mechanism of the motor protein kinesin. This protein has been a particularly rewarding subject of FRET studies because of its processive stepping mechanism, involving the hand-over-hand motion of two identical motor domains, brought about by conformational changes driven by the enzymatic hydrolysis of ATP. In my view applications of FRET to kinesin have not been exhaustive. Not all aspects of kinesin motility involving conformational changes have been resolved and are fully understood. Further single-molecule FRET, with labels on different parts of the proteins and better signal-to-noise and time resolution will surely lead to new insights and further understanding of kinesin motility. Particularly interesting would be experiments combining optical tweezers revealing force generation and overall stepping, and FRET revealing distinct conformational changes that are cause and consequence of stepping. I foresee further applications of FRET to kinesin in living cells or whole organisms, potentially on the single-molecule level addressing for example cargo binding, motor regulation and cooperation between multiple motors. Such studies will benefit from the development of

novel fluorescent probes that are small yet bright and photostable. Many motor proteins other than Kinesin-1 are far less well understood, for example other members of the kinesin superfamily or dyneins. Studies of the mechanisms of these motor proteins will surely be helped by FRET experiments. In my view, FRET, at the single-molecule and ensemble level, is and will remain a crucial technique to reveal structural dynamics in biomolecules. These dynamics are the underlying actors driving protein and polynucleotide function and thus need to be understood in detail.

2.3.11 Acknowledgements

I would like to thank Drs Zdenek Lansky, Bettina Lechner, Sander Verbrugge, Günther Woehlke for their collaboration and discussions on the subject of this chapter. Work the laboratory of Erwin J. G. Peterman is financially supported by a Vici fellowship from the Netherlands Organization for Scientific Research, Physics (NWO-N), by an ALW Open Programme grant from NWO, Earth and Life Sciences (NWO-ALW), an NWO Groot investment grant and is part of the "Barriers in the Brain" research program of the Foundation for Fundamental Research on Matter (FOM), which is financially supported by NWO.

REFERENCES

1. Berg, J. M.; Tymoczko, J. L.; and Stryer, L. *Biochemistry*. 6th ed.; W.H. Freeman: New York, **2007**.

2. Gennerich, A.; and Vale, R. D. Walking the walk: how kinesin and dynein coordinate their steps. *Current Opinion in Cell Biology* **2009**, 21: 59-67.

3. Howard, J., *Mechanics of motor proteins and the cytoskeleton*. Sinauer Associates, Publishers: Sunderland, Mass., **2001**; p xvi, 367 p.

4. Vale, R. D. The molecular motor toolbox for intracellular transport. *Cell* **2003**, 112: 467-480.

5. Block, S. M. Kinesin motor mechanics: Binding, stepping, tracking, gating, and limping. *Biophysical Journal* **2007**, 92: 2986-2995.

6. Moerner, W. E.; and Orrit, M. Illuminating single molecules in condensed matter. *Science* **1999**, 283: 1670-1676.

7. Kapitein, L. C.; and Peterman, E. J. G., Chapter 2 - Single Molecule Experiments and the Kinesin Motor Protein Superfamily: Walking Hand in Hand. In *Single Molecule Biology*, Knight, A., Ed. Academic Press: New York, **2009**; pp 35-60.

8. Svoboda, K.; Schmidt, C. F.; Schnapp, B. J.; and Block, S. M. Direct observation of kinesin stepping by optical trapping interferometry. *Nature* **1993**, 365: 721-727.

9. Visscher, K.; Schnitzer, M. J.; and Block, S. M. Single kinesin molecules studied with a molecular force clamp. *Nature* **1999**, 400: 184-189.

10. Vale, R. D.; Funatsu, T.; Pierce, D. W.; Romberg, L.; Harada, Y.; and Yanagida, T. Direct observation of single kinesin molecules moving along microtubules. *Nature* **1996**, 380: 451-453.

11. Yildiz, A.; Tomishige, M.; Vale, R. D.; and Selvin, P. R. Kinesin walks hand-over-hand. *Science* **2004**, 303: 676-678.

12. Cantor, C. R.; and Schimmel, P. R., *Techniques for the study of biological structure and function*. W. H. Freeman: San Francisco, **1980**; p xxix p., p. 344-846, 351.

13. Valeur, B., *Molecular fluorescence: principles and applications*. Wiley-VCH: Weinheim ; New York, **2002**; p xiv, 387 p.

14. Stryer, L.; and Haugland, R. P. Energy Transfer - a Spectroscopic Ruler. *Proceedings of the National Academy of Sciences of the United States of America* **1967**, 58: 719-726.

15. Forster, T. *Zwischenmolekulare Energiewanderung Und Fluoreszenz. *Annalen der Physik-Berlin* **1948**, 2: 55-75.

16. Lakowicz, J. R., *Principles of fluorescence spectroscopy*. 3rd ed.; Springer: New York, **2006**; p xxvi, 954 p.

17. Kapanidis, A. N.; and Weiss, S. Fluorescent probes and bioconjugation chemistries for single-molecule fluorescence analysis of biomolecules. *The Journal of Chemical Physics* **2002**, 117: 10953-10964.

18. Shaner, N. C.; Steinbach, P. A.; and Tsien, R. Y. A guide to choosing fluorescent proteins. *Nature Methods* **2005**, 2: 905-909.

19. Brasselet, S.; Peterman, E. J. G.; Miyawaki, A.; and Moerner, W. E. Single-molecule fluorescence resonant energy transfer in calcium concentration dependent cameleon. *The Journal of Physical Chemistry B* **2000**, 104: 3676-3682.

20. Clegg, R. M. Fluorescence resonance energy-transfer and nucleic-acids. *Methods in Enzymology* **1992**, 211: 353-388.

21. Kalinin, S.; Peulen, T.; Sindbert, S.; Rothwell, P. J.; Berger, S.; Restle, T.; Goody, R. S.; Gohlke, H.; and Seidel, C. A. M. A toolkit and benchmark study for FRET-restrained high-precision structural modeling. *Nature Methods* **2012**, 9: 1218-1225.

22. Muschielok, A.; Andrecka, J.; Jawhari, A.; Bruckner, F.; Cramer, P.; and Michaelis, J. A nano-positioning system for macromolecular structural analysis. *Nature Methods* **2008**, 5: 965-971.

23. Wozniak, A. K.; Schroder, G. F.; Grubmuller, H.; Seidel, C. A. M.; and Oesterhelt, F. Single-molecule FRET measures bends and kinks in DNA. *Proceedings of the National Academy of Sciences of the United States of America* **2008**, 105: 18337-18342.

24. Ha, T.; Zhuang, X. W.; Kim, H. D.; Orr, J. W.; Williamson, J. R.; and Chu, S. Ligand-induced conformational changes observed in single RNA molecules. *Proceedings of the National Academy of Sciences of the United States of America* **1999**, 96: 9077-9082.

25. Pawley, J. B., *Handbook of biological confocal microscopy*. 3rd ed.; Springer: New York, NY, **2006**; p xxviii, 985 p.

26. Weiss, S. Fluorescence spectroscopy of single biomolecules. *Science* **1999**, 283: 1676-1683.

27. Ha, T.; Enderle, T.; Ogletree, D. F.; Chemla, D. S.; Selvin, P. R.; and Weiss, S. Probing the interaction between two single molecules: Fluorescence resonance energy transfer between a single donor and a single acceptor. *Proceedings of the National Academy of Sciences of the United States of America* **1996**, 93: 6264-6268.

28. Deniz, A. A.; Dahan, M.; Grunwell, J. R.; Ha, T. J.; Faulhaber, A. E.; Chemla, D. S.; Weiss, S.; and Schultz, P. G. Single-pair fluorescence resonance energy transfer on freely diffusing molecules: Observation of Forster distance dependence and subpopulations. *Proceedings of the National Academy of Sciences of the United States of America* **1999**, 96: 3670-3675.

29. Kapanidis, A. N.; Lee, N. K.; Laurence, T. A.; Doose, S.; Margeat, E.; and Weiss, S. Fluorescence-aided molecule sorting: Analysis of structure and interactions by alternating-laser excitation of single molecules. *Proceedings of the National Academy of Sciences of the United States of America* **2004**, 101: 8936-8941.

30. Verbrugge, S.; Lansky, Z.; and Peterman, E. J. G. Kinesin's step dissected with single-motor FRET. *Proceedings of the National Academy of Sciences of the United States of America* **2009**, 106: 17741-17746.

31. Verbrugge, S.; Kapitein, L. C.; and Peterman, E. J. G. Kinesin moving through the spotlight: Single-motor fluorescence microscopy with submillisecond time resolution. *Biophysical Journal* **2007**, 92: 2536-2545.

32. van den Wildenberg, S. M.; Prevo, B.; and Peterman, E. J. A brief introduction to single-molecule fluorescence methods. *Methods in molecular biology* **2011**, 783: 81-99.

33. Schuler, B.; Lipman, E. A.; and Eaton, W. A. Probing the free-energy surface for protein folding with single-molecule fluorescence spectroscopy. *Nature* **2002**, 419: 743-747.

34. Kapanidis, A. N.; Margeat, E.; Ho, S. O.; Kortkhonjia, E.; Weiss, S.; and Ebright, R. H. Initial transcription by RNA polymerase proceeds through a DNA-scrunching mechanism. *Science* **2006**, 314: 1144-1147.

35. Hackney, D. D.; and Jiang, W. Assays for kinesin microtubule-stimulated ATPase activity. *Methods in Molecular Biology* **2001**, 164: 65-71.

36. Cheng, J. Q.; Jiang, W.; and Hackney, D. D. Interaction of mant-adenosine nucleotides and magnesium with kinesin. *Biochemistry-Us* **1998**, 37: 5288-5295.

37. Woodward, S. K. A.; Eccleston, J. F.; and Geeves, M. A. Kinetics of the Interaction of 2'(3')-O-(N-Methylanthraniloyl)-Atp with Myosin Subfragment-1 and Actomyosin Subfragment-1 - Characterization of 2 Acto.S1.Adp Complexes. *Biochemistry-Us* **1991**, 30: 422-430.

38. Umezu, N.; Hanzawa, N.; Yamada, M. D.; Kondo, K.; Mitsui, T.; and Maruta, S. Biochemical characterization of the novel rice kinesin K23 and its kinetic study using fluorescence resonance energy transfer between an intrinsic tryptophan residue and a fluorescent ATP analogue. *The Journal of Biochemistry* **2011**, 149: 539-550.

39. Maliga, Z.; Kapoor, T. M.; and Mitchison, T. J. Evidence that monastrol is an allosteric inhibitor of the mitotic kinesin Eg5. *Chemistry & Biology* **2002**, 9: 989-996.

40. Xing, J.; Wriggers, W.; Jefferson, G. M.; Stein, R.; Cheung, H. C.; and Rosenfeld, S. S. Kinesin has three nucleotide-dependent conformations - Implications for strain-dependent release. *The Journal of Biological Chemistry* **2000**, 275: 35413-35423.

41. Verbrugge, S.; Lechner, B.; Woehlke, G.; and Peterman, E. J. G. Alternating-Site Mechanism of Kinesin-1 Characterized by Single-Molecule FRET Using Fluorescent ATP Analogues. *Biophysical Journal* **2009**, 97: 173-182.

42. Shastry, S.; and Hancock, W. O. Neck Linker Length Determines the Degree of Processivity in Kinesin-1 and Kinesin-2 Motors. *Current Biology* **2010**, 20: 939-943.

43. Arnal, I.; and Wade, R. H. Nucleotide-dependent conformations of the kinesin dimer interacting with microtubules. *Structure* **1998**, 6: 33-38.

44. Rice, S.; Lin, A. W.; Safer, D.; Hart, C. L.; Naber, N.; Carragher, B. O.; Cain, S. M.; Pechatnikova, E.; Wilson-Kubalek, E. M.; Whittaker, M.; Pate, E.; Cooke, R.; Taylor, E. W.; Milligan, R. A.; and Vale, R. D. A structural change in the kinesin motor protein that drives motility. *Nature* **1999**, 402: 778-784.

45. Case, R. B.; Rice, S.; Hart, C. L.; Ly, B.; and Vale, R. D. Role of the kinesin neck linker and catalytic core in microtubule-based motility. *Current Biology* **2000**, 10: 157-160.

46. Rosenfeld, S. S.; Xing, J.; Jefferson, G. M.; Cheung, H. C.; and King, P. H. Measuring kinesin's first step. *The Journal of Biological Chemistry* **2002**, 277: 36731-36739.

47. Tomishige, M.; Stuurman, N.; and Vale, R. Single-molecule observations of neck linker conformational changes in the kinesin motor protein. *Nature Structural & Molecular Biology* **2006**, 13: 887-894.

48. Asenjo, A. B.; Weinberg, Y.; and Sosa, H. Nucleotide binding and hydrolysis induces a disorder-order transition in the kinesin neck-linker region. *Nature Structural & Molecular Biology* **2006**, 13: 648-654.

49. Rice, S.; Cui, Y.; Sindelar, C.; Naber, N.; Matuska, M.; Vale, R.; and Cooke, R. Thermodynamic properties of the kinesin neck-region docking to the catalytic core. *Biophysical Journal* **2003**, 84: 1844-1854.

50. Guydosh, N. R.; and Block, S. M. Backsteps induced by nucleotide analogs suggest the front head of kinesin is gated by strain. *Proceedings of the National Academy of Sciences of the United States of America* **2006**, 103: 8054-8059.

51. Rosenfeld, S. S.; Fordyce, P. M.; Jefferson, G. M.; King, P. H.; and Block, S. M. Stepping and stretching - How kinesin uses internal strain to walk processively. *The Journal of Biological Chemistry* **2003**, 278: 18550-18556.

52. Wang, Z. H.; and Sheetz, M. P. The C-terminus of tubulin increases cytoplasmic dynein and kinesin processivity. *Biophysical Journal* **2000**, 78: 1955-1964.

53. Martin, D. S.; Fathi, R.; Mitchison, T. J.; and Gelles, J. FRET measurements of kinesin neck orientation reveal a structural basis for processivity and asymmetry. *Proceedings of the National Academy of Sciences of the United States of America* **2010**, 107: 5453-5458.

54. Mori, T.; Vale, R. D.; and Tomishige, M. How kinesin waits between steps. *Nature* **2007**, 450: 750-754.

55. Toprak, E.; Yildiz, A.; Hoffman, M. T.; Rosenfeld, S. S.; and Selvin, P. R. Why kinesin is so processive. *Proceedings of the National Academy of Sciences of the United States of America* **2009**, 106: 12717-12722.

56. Hackney, D. D.; Levitt, J. D.; and Suhan, J. Kinesin Undergoes a 9-S to 6-S Conformational Transition. *The Journal of Biological Chemistry* **1992**, 267: 8696-8701.

57. Stock, M. F.; Guerrero, J.; Cobb, B.; Eggers, C. T.; Huang, T. G.; Li, X.; and Hackney, D. D. Formation of the compact confomer of kinesin requires a COOH-terminal heavy chain domain inhibits microtubule-stimulated ATPase activity. *The Journal of Biological Chemistry* **1999**, 274: 14617-14623.

58. Hackney, D. D.; and Stock, M. F. Kinesin's IAK tail domain inhibits initial microtubule-stimulated ADP release. *Nature* **2000**, 2: 257-260.

59. Hackney, D. D.; Baek, N.; and Snyder, A. C. Half-Site Inhibition of Dimeric Kinesin Head Domains by Monomeric Tail Domains. *Biochemistry-Us* **2009**, 48: 3448-3456.

60. Cai, D. W.; Hoppe, A. D.; Swanson, J. A.; and Verhey, K. J. Kinesin-1 structural organization and conformational changes revealed by FRET stoichiometry in live cells. *The Journal of Cell Biology* **2007**, 176: 51-63.